Indian Journal of Chemistry
Vol. 65, February 2026, pp. 135-144
DOI: 10.56042/ijc.v65i2.24806

Synthesis and structural studies of Mn(II) and Zn(II) thiazole–Schiff base complexes with catalytic application in benzyl alcohol oxidation

Gurdeep Sangwan[a], Jyoti Sharma*[a], Sonu Prasad[a] & Vikas Rathod[b]

[a] Department of Chemistry, MMEC, Maharishi Markandeshwar (Deemed to be University), Mullana 133 207, Haryana, India

[b] IOL Chemicals and Pharmaceuticals, Barnala 148 101, Punjab, India

E-mail: jsharma117@gmail.com

Received 22 October 2025; accepted (revised) 3 February 2026

Manganese (II) and zinc(II) Schiff base complexes derived from salicylaldehyde and Ethyl 2-(2-amino-1,3-thiazol-4-yl)acetate have been synthesized and characterized using elemental analyses, IR and UV-Vis spectroscopy. Their catalytic activities have been assessed for the selective oxidation of benzyl alcohol employing hydrogen peroxide as a green oxidant under mild conditions. The gas chromatographic study has identified benzaldehyde as the primary product, with benzoic acid and benzyl benzoate as minor by-products. The manganese complex exhibits the superior catalytic activity, (approximately 95% selectivity) due to its redox versatility and enhanced electron-transfer capability. The study demonstrates that optimization of parameters such as reaction time, temperature, H_2O_2 concentration, catalyst loading, and catalyst type significantly influences both selectivity and conversion. With a selectivity of approximately 95%, this reaction is particularly promising for industrial applications in benzyl alcohol oxidation using environmentally benign catalysts.

Keywords: Schiff base, Metal complexes, Catalytic oxidation, Benzyl alcohol

Schiff bases, derived from the condensation of primary amines with carbonyl compounds[1], have garnered significant attention in coordination chemistry due to their versatile ligand properties and ability to stabilize metal ions in various oxidation states. Their inherent structural flexibility, combined with the presence of nitrogen and oxygen donor atoms especially aromatic aldehyde Schiff bases, makes them ideal candidates for forming stable metal complexes[2]. These metal complexes exhibit a wide range of biological and catalytic activities, making them attractive for applications in fields such as biochemistry, materials science, and catalysis[3,4].

Schiff base metal complexes are renowned for their exceptional catalytic properties, attributed to their customizable characteristics, resilience under various conditions, and adaptable coordination chemistry. The structural versatility of Schiff base ligands allows for precise modification of electronic and steric attributes, enabling the development of catalysts with tailored reactivity and selectivity[5]. These complexes exhibit significant stability across diverse reaction environments, ensuring durability and consistent performance[6]. Their flexible coordination geometry facilitates the formation of well-defined metal centers capable of activating substrates and stabilizing reaction intermediates. Schiff base metal complexes demonstrate catalytic proficiency in numerous organic transformations, including oxidation[7], reduction[8], epoxide ring opening[9], and carbon-carbon bond formation reactions[10], underscoring their broad applicability in organic synthesis.

Among the diverse catalytic applications of Schiff base metal complexes[11], oxidation reactions have been extensively studied due to their industrial relevance. Catalytic oxidation processes, especially those that involve the transformation of alcohols into corresponding aldehydes, are of particular importance in the fine chemical and pharmaceutical industries. Benzyl alcohol oxidation, for instance, is a key reaction in organic synthesis, yielding benzaldehyde, which is a valuable intermediate in the production of perfumes, dyes, and flavoring agents[12].

In this study, we report the synthesis of a Schiff base derived from 2-hydroxybenzaldehyde and its zinc and manganese metal complexes. These complexes were thoroughly characterized using spectroscopic techniques such as IR, UV-Vis, and ^{1}H and ^{13}C NMR, along with elemental analysis. Manganese is well-known for its ability to participate in redox reactions, often cycling between different oxidation states during catalysis[13]. We then evaluated the catalytic performance of these

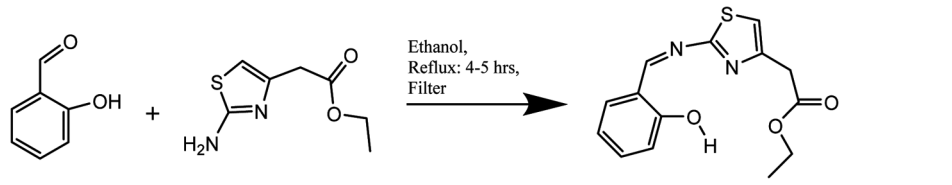

Salicylaldehyde Ethyl 2-amino-4-thiazoleacetate (*Z*)-ethyl 2-(2-((2-hydroxybenzylidene)amino)thiazol-4-yl)acetate

Scheme 1 — Synthesis of Schiff base ligand

complexes in the oxidation of benzyl alcohol under varying conditions, including solvents, catalyst load, oxidant-to-substrate ratio, and temperature. The goal of this work is to investigate the catalytic efficiency and selectivity of these complexes, as well as to compare the activities of the zinc and manganese complexes in promoting the oxidation of benzyl alcohol.

Experimental Section

All the chemicals were used as received without further purification. Salicylaldehyde (Sigma-Aldrich), Ethyl 2-(2-amino-1,3-thiazol-4-yl)acetate (TCI chemicals), Zinc (II) acetate dihydrate (Lobachemie Limited), Manganese (II) acetate tetrahydrate (Lobachemie Limited), Ethanol (CSS), Acetonitrile (RANKEM), DMF (RANKEM), DMSO (RANKEM), H_2O_2 (50%) (RX Chemicals). Reaction monitoring was done by GC (Agilent) by using GC method A (column: HP-5MS 30m*0.25mm*0.25u, Injector mode: split, Split temp = 220°C, Carrier gas: N_2, Column Flow: 3.5 mL/min, Split Ratio: 1:20, Injection Volume: 0.2 µL, Detector: FID, Detector temperature: 230°C, H_2 Flow: 40 mL/min, Air Flow: 400 mL/min, N_2 (for makeup): 25 mL/min, Run Time: About 15.9 min) and GC method B (J&W DB-WAX GC 30 m*0.53 mm*1.00 µm, Injector mode: split, Split temp = 250°C, Carrier gas: N_2, Column Flow: 1.0 mL/min, Split Ratio: 13:1, Injection Volume: 0.5 µL, Detector: FID, Detector temperature: 250°C, H_2 Flow: 40 mL/min, Air Flow: 400 mL/min, N_2 (for makeup): 10 mL/min, Run Time: 25 min).

IR was done by using Shimadzu FT-IR, ^{1}H and ^{13}C NMR were done by using BRUKER Advance Neo 500 MHz NMR spectrometer. TGA 550 was used for TGA and Shimadzu UV-1900i was used for UV-Vis spectroscopy. Waters Xevo TQ-S Micro LC-MS/MS was used for mass spectroscopy.

Synthesis of Schiff base ligand(L) *i.e.* (Z)-ethyl 2-(2-((2-hydroxybenzylidene)amino)thiazol-4-yl) acetate)

Salicylaldehyde (5.0 g, 0.04 mol) and ethyl 2-(2-amino-1,3-thiazol-4-yl)acetate (7.63 g, 0.04 mol) were mixed in 30 mL of ethanol and refluxed for 4-5 hours (Scheme 1). The reaction was monitored by TLC (mobile phase- MDC:Methanol: 0.5: 9.5), and a yellow solid precipitated, which was filtered, washed with hot ethanol, and recrystallized from ethanol. The product was dried in a vacuum at 50°C for 6 hours. Yield 7.0 g (59%). FT-IR (KBr): 3425.59 (O–H,Hydroxy group), 3120.96 (C–H stretching, Alkene), 2890.0 (C–H stretching, Methyl), 1722.85 (C=O stretching, Ester), 1610.77 (C=N stretching, Ring); 1571.98 (C=N stretching, azomethine), 1523.21 (C=C stretching, cyclic alkene), 750.07 (C–H out-of-plane bending), 721.0 cm^{-1} (C–S stretching); UV-Vis (MeOH, λmax, nm, log ε): 210 (0.73), 225 (0.40), 236.5 (0.49), 253 (0.20), 274.5 (0.33), 366 (0.68); ^{1}H NMR (500 MHz, DMSO-d_6): δ 1.2098–1.2382 (3H, t, $–CH_3$), 3.8292 (2H, s,$–CH_2$), 4.1162–4.1588 (2H, q,$–OCH_2$), 6.9807–7.0278 (2H, d,–Ar–H), 7.4353 (s, 1H, –Ar–H), 7.4633–7.4977 (1H, t,–Ar–H), 7.8524–7.8712 (1H, d,–Ar–H), 9.2890 (1H, d,–NH), 11.5900 (1H, s,–OH); ^{13}C NMR (500 MHz, DMSO-d_6): δ 170.03, 169.79, 163.14, 160.15, 147.46, 134.75, 131.27, 119.62, 119.36, 116.73, 116.38, 60.39, 36.64,13.97; ESI-MS (positive mode): *m/z* 291.05 $[M+H]^+$.

Synthesis of Manganese Schiff base Complex

5 g (0.017mol) Schiff base, and Methanol 30 mL was taken in a 1-n RBF and heated to 60°C to get a clear solution. To the clear solution, hot solution of Manganese acetate tetrahydrate [4.2 g (0.017 mol) in 30 mL methanol] was added. The reaction was maintained for 4 hours at 60°C and then solid precipitated in the form of metal complex (Scheme 2). The product was filtered, washed with hot methanol followed by hexane and recrystallized from MeOH and dried in oven at 50°C for 4 hours.

Yield 2.5 g (41.32%). FT-IR (KBr): 3103 (O–H, coordinated water), 1653 ($COO^–$ asymmetric), 1600 (C=N, imine), 1553 (C=N, ring), 1444 ($COO^–$ symmetric), 1287 (C–O, phenolic), 609 (Mn–O), 485 cm^{-1} (Mn–N); UV-Vis (solid state, λmax, nm, log ε):

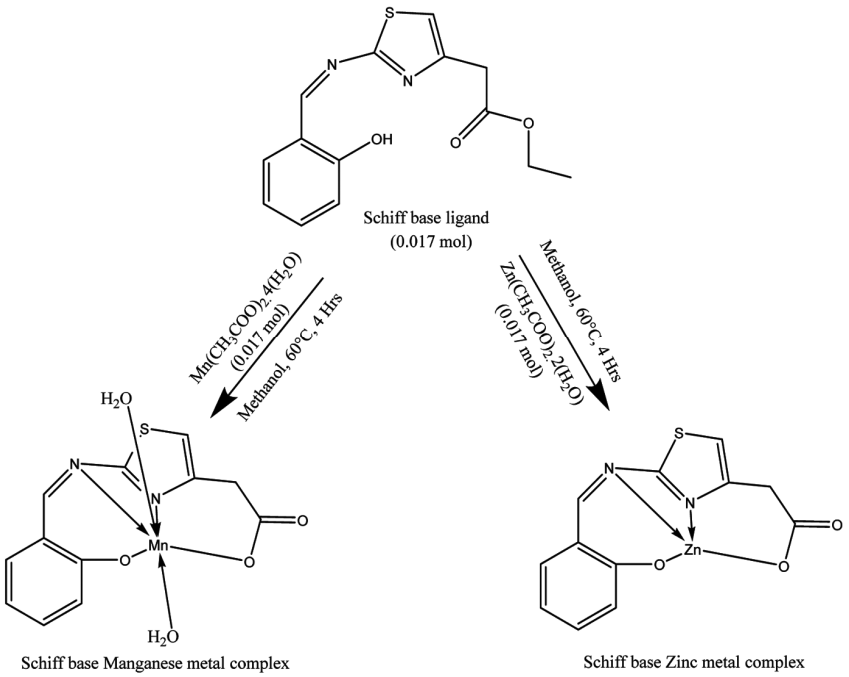

Scheme 2 — Synthesis of MnL and ZnL metal complexes

259.5 (0.403), 352 (0.152), 541.5 (0.037). Anal. Calcd: C, 40.84; H, 3.40; N, 7.77; S, 9.01; O, 23.54; Mn, 15.44. Found: C, 41.03; H, 3.44; N, 7.98; S, 9.13; O, 22.78; Mn, 15.64%.

Synthesis of Zinc metal complex

Schiff base (5 g, 0.017mol) and methanol (30 mL) was taken in 1-n RBF and heated to 60°C to get a clear solution followed by the addition of hot methanolic solution of zinc acetate dihydrate (3.8 g, 0.017 mol). The reaction was maintained at 60°Cfor 4 hours (Scheme 2). The obtained solid was filtered out and washed with hot methanol followed by hexane wash. The solid material was dried in oven at 50°C for 4 hours.

Yield: 2.7 g (48.12%). FT-IR (KBr): 3103 (O–H, coordinated water), 1638 (COO^- asymmetric), 1580 (C=N, imine), 1566 (C=N, ring), 1413 (COO^- symmetric), 1293 (C–O, phenolic), 580 (Zn–O), 436 cm^{-1} (Zn–N); UV-Vis (solid state, λmax, nm, log ε): 256 (0.642), 351.5 (0.192); ESI-MS (positive mode): *m/z* 326 $[M+H]^+$. Anal. Calcd: C, 44.26; H, 2.23; N, 8.92; S, 10.18; O, 13.65; Zn, 20.08. Found: C, 44.11; H, 2.23; N, 8.92; S, 10.18; O, 13.65; Zn, 20.55%.

General procedure for catalytic oxidation of benzyl alcohol

5.0 g (46 mmol) of substrate, 25 mL DMF/DMSO, 6.28 g (92.4mmol) H_2O_2 (50% w/w) and 0.25 g catalyst were taken in single neck RBF (Scheme 3).

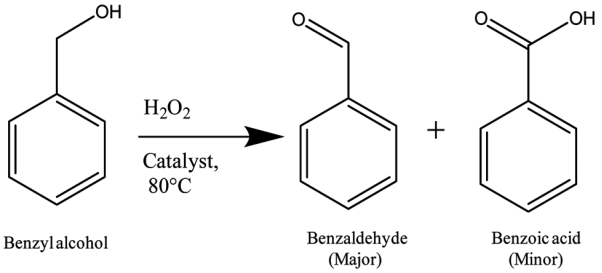

Scheme 3 — General conditions for catalytic oxidation of benzyl alcohol

The reaction mixture was heated to 80°C. Samples were withdrawn after 4, 8 and 12 hours for GC reaction monitoring.

Sample preparation

1 mL of sample was withdrawn every time which was added with pinch of MnO_2 to quench excess H_2O_2. Thereafter, a small amount of anhydrous Na_2SO_4 was added to remove residual water from the sample. After filtration to separate the Na_2SO_4, the resulting filtrate was subjected to gas chromatography (GC) analysis[14].

Result and Discussions

Characterization of ligand

LCMS

A high-density peak at 291.05 (M+1) corresponding to the protonated molecular ion,

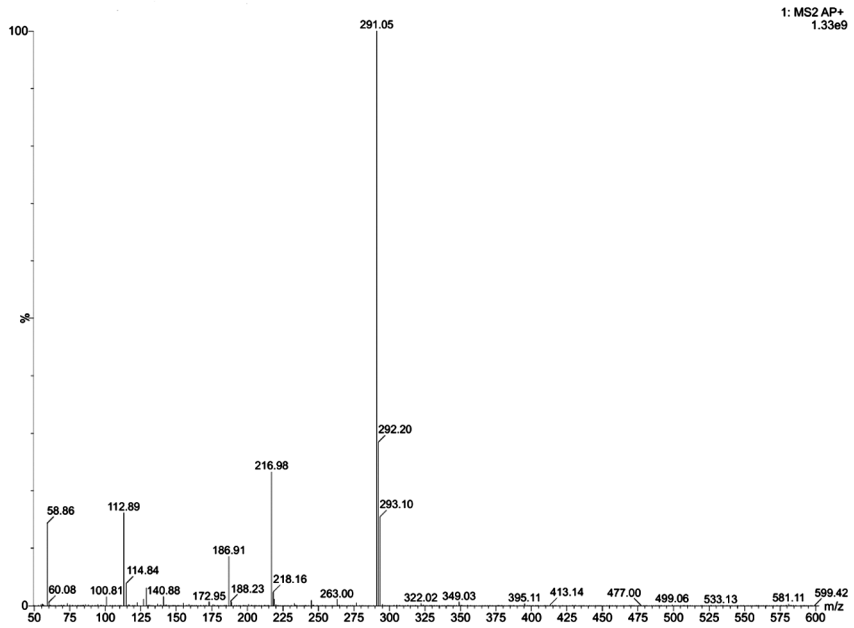

Fig. 1 — LCMS spectra of Schiff base ligand

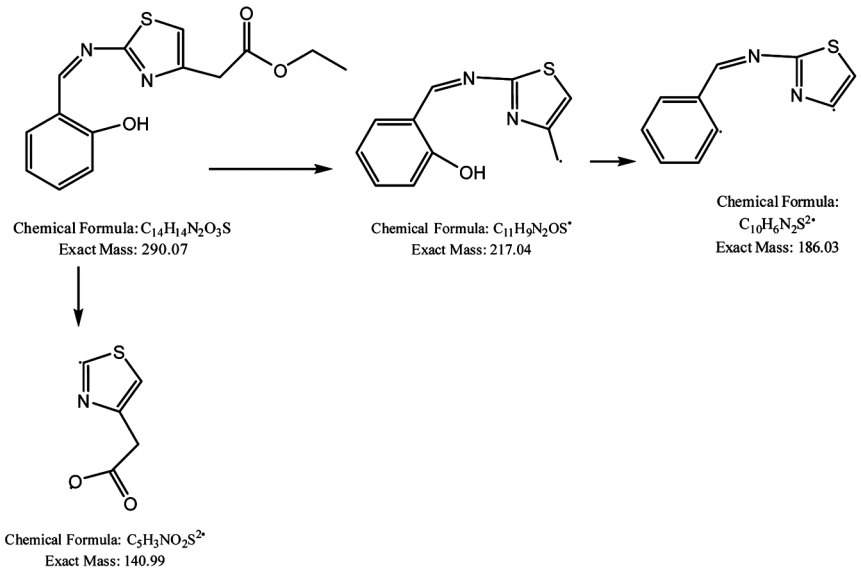

Fig. 2 — Mass fragmentations of Schiff base ligand

confirming the molecular weight of the compound. Peak at 216.98 is likely a fragment resulting from cleavage of the ester moiety and peak at 186.91 is the secondary fragment. 140.88 resulted from loss of ethyl group and $C_7H_6NO^{\bullet}$ (Fig. 1). The possible mass fragmentation pattern is shown in Fig. 2.

IR

The IR spectrum of the Schiff base ligand confirms the presence of key functional groups. A broad O-H stretching vibration at 3425 cm^{-1} indicates a phenolic hydroxyl group[15]. The strong peak at 1722 cm^{-1} corresponds to the ester (C=O) group. The imine (C=N) stretching at 1610 cm^{-1} confirms Schiff base formation and a ring C=N vibration appears at 1571 cm^{-1}, and C-O stretching of the hydroxyl group is observed at 1278 cm^{-1} (Fig. 3)[16].

Characterization of Manganese metal complex

In the Schiff base ligand, the O-H stretch at 3425 cm^{-1} is not detected in the MnL complex, suggesting deprotonation or participation in

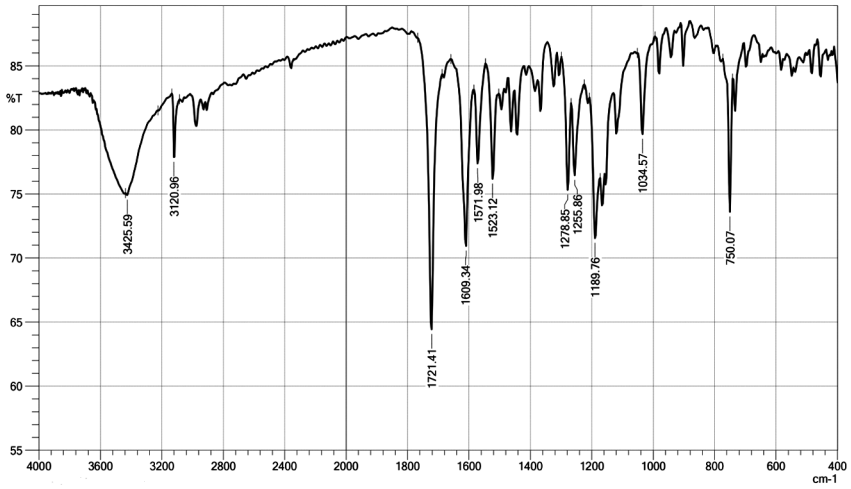

Fig. 3 — IR spectrum of Schiff base ligand

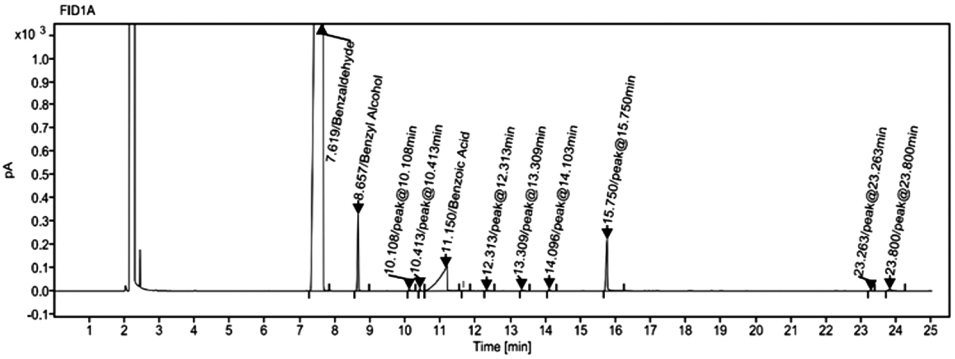

Fig. 4 — GC reaction monitoring data with 20% w/w MnL catalyst and Acetonitrile as solvent

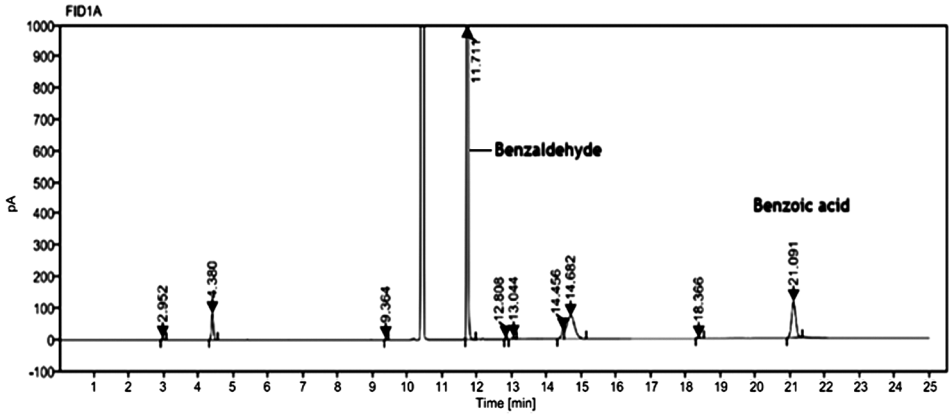

Fig. 5 — GC reaction monitoring data with 5% w/w MnL catalyst and DMF as solvent

coordination. The C-O stretching vibration shifting from 1278 cm^{-1} to 1298 cm^{-1} also supports coordination *via* phenolic OH. The ethyl ester group hydrolyses to acid which is supported by GC analysis of reaction mixture (Fig. 4 and Fig. 5) which shows ethanol formation in the reaction. Consequently, the carbonyl (C=O) stretching peak of the ester at 1721 cm^{-1} is not detected in the spectrum of the complex. Instead, new peaks appear at 1620 cm^{-1} (asymmetric stretch) and 1413 cm^{-1} (symmetric stretch), which are characteristic of a carboxylate group ($-COO^{-}$). The difference between the asymmetric and symmetric stretching frequencies (>200 cm^{-1}) suggests monodentate coordination of the

Table 1 — IR vibrational frequencies of ligand (L), ZnL complex and MnL complex

Functional Group	Schiff Base Ligand (cm^{-1})	ZnL Complex (cm^{-1})	MnL Complex (cm^{-1})
O-H (Hydroxyl)	3425	Not detected	Not detected
O-H (Water)	Not present	Not present	3304 (Coordinated water)
C=O (Ester)	1722	1638 (COO^- Asymmetric)	1620 (COO^- Asymmetric)
C=N (Imine)	1610	1580	1551
C=N (Ring)	1571	1566	1517
COO^- Symmetric stretch	Not detected	1413	1413
C-O (Stretching OH group)	1278	1293	1298
Zn-O	Not present	580	Not present
Zn-N	Not present	436	Not present
Mn-O	Not present	Not present	678
Mn-N	Not present	Not present	413

-COO^- group. The in-plane and out-of-plane bending modes of the -COO^- group are observed at 724 cm^{-1} and 678 cm^{-1}, respectively. The imine C=N band at 1610 cm^{-1} shifts to 1557 cm^{-1}, shows coordination of the imine nitrogen to the Mn centre. New bands at 678 cm^{-1} (Mn-O) and 413 cm^{-1} further validate the metal-ligand bonding. The shift in IR frequencies of MnL with respect to the ligand (L) upon metalation is shown in Table 1. Additionally, the O-H stretch at 3304 cm^{-1} in the complex might correspond to coordinated molecules of water (Fig. 6)[17]. The UV-Vis spectrum of the MnL complex shows three key features corresponding to different electronic transitions (Fig. 7). The strong peak at 259.5 nm (Absorbance: 0.403) may be due to π-π* transitions, arising from the conjugated π-electron system in the Schiff base ligand, including aromatic rings and the azomethine group. The moderate peak at 352.0 nm (Absorbance: 0.152) can be attributed to n-π* transitions involving lone pairs on oxygen or nitrogen atoms transitioning to π* orbitals. The weak and broad band around 541.5 nm (Absorbance: 0.037) may be due to a d-d transition or possibly a ligand-to-metal charge transfer (LMCT)[18]. The spectral data indicates the formation of an octahedral complex. TGA reveals an initial 11.02% weight loss up to 120°C, attributed to two coordinated water molecules, followed by major decomposition (86.09%) between 200–600°C (Fig. 8). The thermal profile confirms moderate stability up to 215°C and supports the octahedral structure of the complex.

Characterization of Zinc metal complex

The IR spectrum of the zinc complex shows significant shifts, confirming structural transformations upon coordination. The imine (C=N)

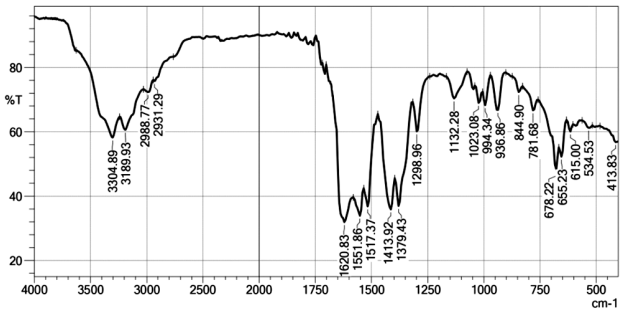

Fig. 6 — IR spectrum of MnL

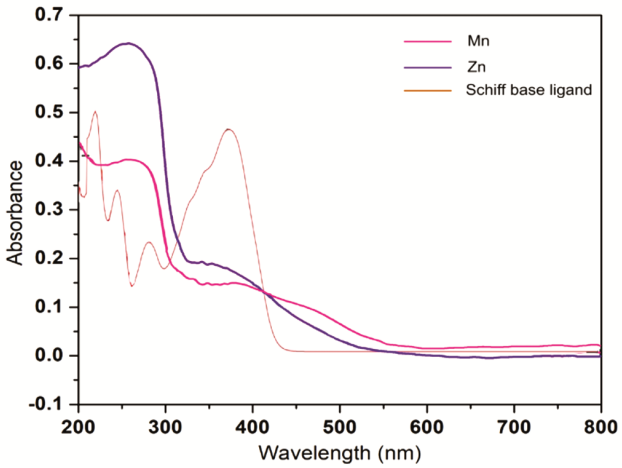

Fig. 7 — UV-Vis Spectral Analysis of Schiff Base ligand (L) and MnL and ZnL Complexes

stretching vibration shifts lower from 1609.34 cm^{-1} in the Schiff base to 1582.03 cm^{-1}, indicating imine nitrogen coordination with Zn. The ring C=N stretch also shifts from 1571.98 cm^{-1} to 1566.23 cm^{-1}. The phenolic O–H peak at 3425 cm^{-1} disappears, suggesting deprotonation and involvement in coordination. The C–O stretch shifts from 1278 cm^{-1} to 1293 cm^{-1}, reflecting electronic changes due to

complexation[19]. The ester carbonyl peak at 1721 cm^{-1} is absent, with new COO^- peaks at 1638 cm^{-1} (asymmetric) and 1413.92 cm^{-1} (symmetric), confirming ester hydrolysis and carboxylate coordination. The COO^- bending vibrations at 724.20 cm^{-1} and 678.22 cm^{-1} further support this. The absence of methyl C–H stretching peaks around 2900 cm^{-1}, along with GC analysis showing ethanol, confirms ester hydrolysis. The shift in IR frequencies of ZnL with respect to the ligand (L) upon metalation is shown in Table 1. Peaks at 580.51 cm^{-1} and 436.82 cm^{-1} correspond to Zn–O and Zn–N bonds, confirming coordination (Fig. 9)[20,21]. The UV-Vis spectrum reveals significant electronic transitions supporting ligand coordination. The peak at 256 nm (absorbance 0.642) corresponds to π-π* transitions from aromatic rings or conjugated systems, while the peak at 351.5 nm (absorbance 0.192) is attributed to n-π* transitions due to heteroatom lone pair interactions. The absence of d–d transitions align with Zn d^{10} electronic configuration, indicating tetrahedral geometry (Fig. 7)[22]. TGA analysis shows an initial weight loss of 1.5805% up to 105°C due to lattice moisture or solvent evaporation, confirming no coordinated water. The complex remains stable between 105°C and 180°C, with significant thermal degradation beginning after 180°C, indicating decomposition beyond this temperature (Fig. 10). The formation of ZnL is also supported by mass spectra, where [M+H+] lies at 326.23 and confirms the mass of the complex.

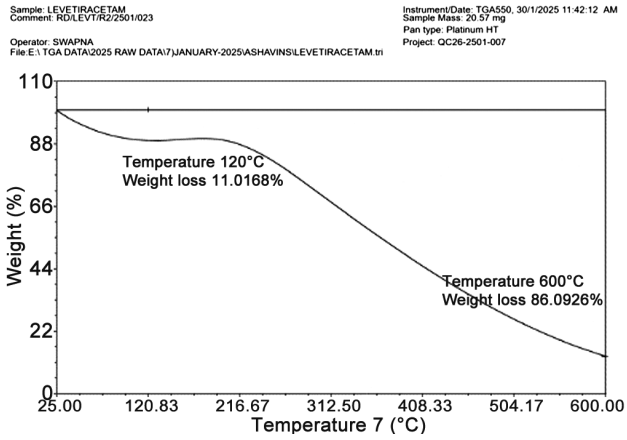

Fig. 8 — TGA analysis of MnL metal complex

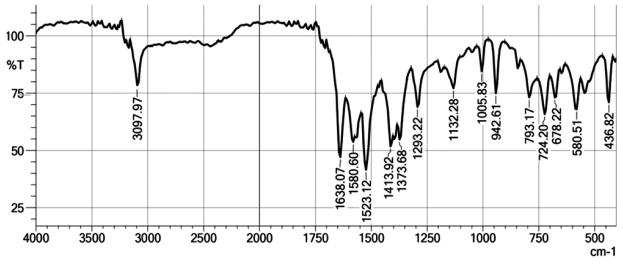

Fig. 9 — IR spectrum of ZnL

Catalytic oxidation of benzyl alcohol

The catalytic oxidation of benzyl alcohol was studied with four variables: temperature (50°C and 80°C), catalyst load (5%, 10%, 20% and 30%), solvents (acetonitrile, DMF and DMSO) and amount of H_2O_2 (1.5, 1.8, 2 and 3 mole equivalents) with both catalysts.

Impact of temperature

The reaction was found to be temperature dependent. For both of the catalysts: ZnL and MnL, maximum oxidation took place at 80°C.At 50°C, the reaction conversion was less in the same span of time as compared to that of 80°C (Table 2, entries:2h,2k; 2mm, 2pp).

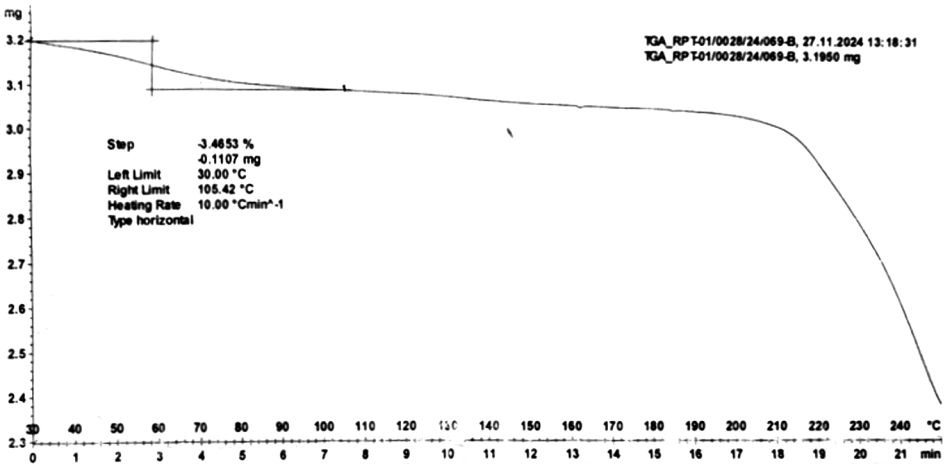

Fig. 10 — TGA analysis of ZnL metal complex

Table 2 — GC reaction monitoring data of oxidation of benzyl alcohol at 50°C and 80°C

Compound	Temp. (°C)	H_2O_2 (mole equivalents)	Time (h)	Solvent	Catalyst	Catalyst Loading (w/w %)	Benz aldehyde (%)	Benzoic Acid (%)	Benzyl Alcohol (%)
2a	80	2	4	Acetonitrile	ZnL	10	33.72	1.34	63.58
2b			8				51.26	3.51	41.89
2c			12				61.79	4.35	29.18
2d			4*				–	–	–
2e			8		MnL	10	86.28	7.07	6.47
2f			12				86.78	10.45	2.60
2g			4				47.05	2.96	46.57
2h			8		ZnL	20	60.00	6.71	26.06
2i			12				67.72	8.27	19.90
2j			4				76.05	3.20	20.68
2k			8[9]		MnL	20	94.73	2.82	1.13
2l			12				87.15	12.72	0.02
2m[#]			8		MnL	30	86.37	13.09	Not detected
2n			4				38.04	1.43	58.6
2o			8		ZnL	10	58.15	3.98	33.11
2p			12				69.22	7.89	18.16
2q			4*				–	–	–
2r			8		MnL	10	84.83	12.41	2.67
2s	80	3	12	Acetonitrile			80.85	17.47	0.57
2t			4				46.26	4.03	46.53
2u			8		ZnL	20	62.27	9.55	18.78
2v			12				69.70	13.50	11.79
2w			4				67.67	7.88	22.14
2x			8		MnL	20	73.46	21.74	Not detected
2y			12				65.2	31.37	Not detected
2z[#]			8	DMF	MnL	5	87.85	6.13	Not detected
2aa[#]			8		MnL	10	91.41	3.12	Not detected
2bb[#]			8	DMSO	MnL	5	89.79	3.68	4.73
2cc[#]			8		MnL	10	87.19	7.14	1.82
2dd[#]			12	DMF	ZnL	5	63.12	1.41	32.79
2ee[#]			12		ZnL	10	55.11	3.19	29.02
2ff[#]			12	DMSO	ZnL	5	56.33	2.23	29.31
2gg[#]			12		ZnL	10	59.53	2.62	25.84
2hh[#]	80	1.5	4	DMF	MnL	5	66.89	2.65	26.51
2ii[#]			8			5	80.70	3.04	14.49
2jj[#]		1.8	4			5	86.98	3.31	7.16
2kk[#]			8[10]			5	94.81	2.49	0.91
2ll	50	2	4	Acetonitrile			21.71	3.21	72.83
2mm			8		ZnL	20	29.85	4.18	62.75
2nn			12				34.31	7.48	54.34
2oo			4				40.00	4.84	55.05
2pp			8		MnL	20	52.00	7.25	42.00
2qq			12				47.09	12.17	39.27
2rr			4				24.99	3.25	65.92
2ss			8		ZnL	20	34.64	4.96	56.02
2tt		3	12				42.53	7.35	45.39
2uu			4				51.27	8.56	36.38
2vv			8		MnL	20	52.71	15.08	29.39
2ww			12				45.51	26.41	23.40

***:**Samples were not analyzed.

9,10: GC chromatograms in Fig. 4 and Fig. 5 respectively.

[#]: GC analytical method is different for these samples analysis.

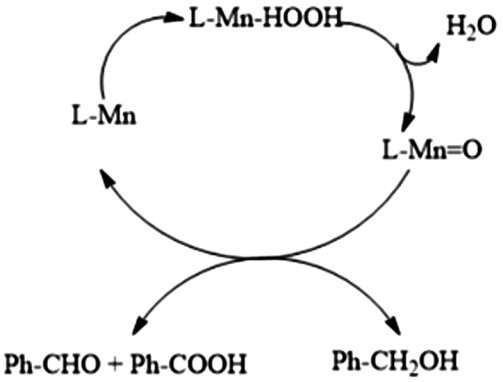

Fig. 11 — Plausible mechanism of reaction of MnL catalyst

Impact of catalyst

Out of the two catalysts, the MnL catalyst was found to show fast reaction conversion and more selective towards benzaldehyde formation. In DMF, at 5% catalyst loading and 2 mole equivalents of 50% H_2O_2 at 80°C, the total reaction conversion to benzaldehyde for MnL catalyst was 89.79%. In case of the ZnLcatalyst, under similar reaction conditions, only 63.12% of benzaldehyde was formed with 32.79% unreacted benzyl alcohol (Table 2, entries: 2bb#; 2dd#).

Impact of catalyst loading

In both catalysts used with acetonitrile as solvent, the total reaction conversion increased when the catalyst amount was doubled from 10% w/w to 20% w/w (Table 2, entries: 2c,2i;2e,2k). However, no significant impact was observed when the catalyst was increased from 20% w/w to 30% w/w (Table 2: entry 2m). Apart from this, one observation was notable that selectivity towards benzaldehyde decreased when the amount of catalyst was increased along with H_2O_2 (2M to 3M) (Table 2, entries:2l,2y) in case of MnL catalyst. In the case of DMF and DMSO as solvents, nearly the same reaction conversions were observed with 5% and 10% of catalyst loadings for both catalysts, which shows that only 5% of catalyst is sufficient (Table 2, entries:2z#;2aa#; 2dd#,2ee#). No reaction conversion was observed in the absence of catalyst.

Impact of quantity of oxidant

When 3 mole equivalents of H_2O_2 was used, despite increase in reaction conversion, the selectivity towards benzaldehyde decreased in case of both of the catalysts. With increase in amount of H_2O_2, the formation of benzoic acid increased due to further oxidation of benzaldehyde (Table 2, entries: 2i, 2v: 2l, 2y). 1.5 mole equivalent of H_2O_2 was not found to be sufficient for maximum conversion and 1.8 mole equivalents of H_2O_2 was found be the optimum quantity (Table 2, entries: 2ii$^{\#}$: 2kk$^{\#}$).

Impact of reaction time

Although Mn catalyst showed more efficiency by showing more reaction conversion, it was observed that with time due to over oxidation benzaldehyde was getting converted to benzoic acid in case of Mn catalyst irrespective of the quantity of oxidant (Table 2, entries: 2e, 2f; 2k,2l; 2r,2s; 2x,2y). The same case was not observed for the Zn catalyst where the selectivity towards benzaldehyde was not impacted with the progress of the reaction (Table 2, entries: 2b, 2c; 2h,2i; 2o,2p; 2u,2v).

Impact of solvent

DMF and DMSO emerged as the most suitable solvents for the Mn catalyst, offering maximum reaction conversion and high selectivity toward benzaldehyde with minimal catalyst usage (Table 2, entries 2z$^{\#}$–2kk$^{\#}$). While acetonitrile also provided good reaction conversions, the catalyst was heterogeneous under the given reaction conditions, necessitating a higher catalyst load to achieve optimal conversion. In contrast, the catalyst was completely soluble in DMF and DMSO, contributing to their efficiency as reaction solvents. The possible mechanism of action of Mn catalyst is presented in Fig. 11.

Conclusion

This study reports the successful synthesis and characterization of novel heterogeneous zinc and manganese Schiff base complexes derived from 2-hydroxybenzaldehyde and ethyl 2-(2-amino-1,3-thiazol-4-yl)acetate. The structural analysis suggests tetrahedral geometry for the zinc complex and octahedral geometry for the manganese complex, as evidenced by IR, UV-Vis, and elemental analysis. Catalytic performance evaluations revealed that both complexes effectively facilitated the selective oxidation of benzyl alcohol to benzaldehyde, with the manganese complex exhibiting superior activity due to its redox versatility and faster reaction kinetics. Reaction conditions such as solvents, temperature, catalyst loading, and oxidant-to-substrate ratio were optimized to maximize conversion and product

selectivity. Notably, the manganese complex showed more selectivity toward benzaldehyde at 80°C with 5% catalyst loading, while the zinc complex was found to be less efficient. These findings highlight the practical applicability of the synthesized complexes in sustainable oxidation processes without requiring hazardous oxidants and establish their potential as environmentally benign and cost-effective catalysts for industrial-scale alcohol oxidation.

Supplementary Information

Supplementary information is available in the website https://nopr.niscpr.res.in/ handle/123456789/ 58776.

Acknowledgments

The authors extend their heartfelt thanks to the Department of Chemistry, Maharishi Markandeshwar (Deemed to be University), Mullana (Ambala), Haryana, India, for their invaluable support and also express gratitude to IOL Chemicals and Pharmaceuticals for their contribution to the successful completion of this research.

References

1 Schiff H, *Just Liebigs Ann Chem*, 131 (1864) 118.
2 Rani A, Sharma J, Ramasamy S K, Saini R V, Khanna R & Sharma E, *Chem Sel*, 10 (2025) e02737.
3 Uddin N, Rashid F, Ali S, Tirmizi S A, Ahmad I, Zaib S, Zubair M, Diaconescu P L, Tahir M N & Iqbal J, *J Biomol Struct Dyn*, 38 (2020) 3246.
4 Nawaz ShariffS, Saravu S & Ramakrishna D, *Schiff Base in Organic, Inorganic and Physical Chemistry*, edited by Akitsu T, (Intech Open, London) 2022, p.7.
5 Dalia S A, Afsan F, Hossain S, Zakaria C & Ali M, *Int J Chem Stu*, 6 (2018) 2859.
6 Gupta K C & Sutar A K, *Coord Chem Rev*, 252 (2008) 1420.
7 Silva A R, Mourao T & Rocha J, *Cat Today*, 203 (2013) 81.
8 Buldurun K, Turan N, Savcı A & Çolak N, *J Saudi Chem Soc*, 23 (2019) 205.
9 Shameli A, Raeisi A H, Pourhasan B, Naeimi H & Ghanbari M M, *Orient J Chem*, 28 (2012) 749.
10 Iyer S, Kulkarni G M & Ramesh C, *Tetrahedron*, 60 (2004) 2163.
11 Akbari A, Amini M, Tarassoli A, Eftekhari-Sis B, Ghasemian N & Jabbari E, *Nano-Struc Nano-Objects*, 14 (2018) 19.
12 Das A & Banik B K, *Microwaves in Chemistry Applications*, (Elsevier, Amsterdam) (2021) p. 205.
13 Ghosh S K, *ACS Omega*, 5 (2020) 25493.
14 Abdel Aziz A A, Salem A N M, Sayed M A & Aboaly M M, *J Mol Struc*, 1010 (2012) 130.
15 Mishra A P & Jain R K, *J Saudi Chem Soc*, 18 (2014) 814.
16 El-Ghamry M A, Elzawawi F M, Aziz A AA, Nassir K M & Abu-El-Wafa S M, *Sci Rep*, 12 (2022) 17942.
17 Aggoun D, Messasma Z, Bouzerafa B, Berenguer R, Morallon E, Ouennoughi Y & Ourari A, *J Mol Struc*, 1231 (2021) 129923.
18 Devi J, Yadav M, Kumar D, Naik L S & Jindal D K, *Appl Organomet Chem*, 33 (2019) e4693.
19 Nair M S, Arish D & Joseyphus R S, *J Saudi Chem Soc*, 16 (2012) 83.
20 Zelenak V, Vargova Z & Gyoryova K, *Spectrochim Acta A Mol Biomol Spect*, 66 (2007) 262.
21 Pardaeva D, Tavman A, Gürbüz D, Hacioglu M, Yilmaz F N, Şahin O, Birteksoz Tan A S & Çinarli A, *Rev Roum Chim*, 69 (2024) 83.
22 Di Nicola C, Karabach Y Yu, Kirillov A M, Monari M, Pandolfo L, Pettinari C & Pombeiro A J L, *Inorg Chem*, 46 (2007) 221.